

Original Paper

Cytotoxic Effects Caused by Functionalized Carbon Nanotube in Murine Macrophages

Krissia Franco de Godoy^a Joice Margareth de Almeida Rodolpho^a
Bruna Dias de Lima Fragelli^a Luciana Camillo^a Patrícia Brassolatti^a
Marcelo Assis^b Camila Tita Nogueira^c Carlos Speglich^d Elson Longo^e
Fernanda de Freitas Anibal^a

^aLaboratório de Inflamação e Doenças Infecciosas, Departamento de Morfologia e Patologia, Universidade Federal de São Carlos, São Carlos, Brazil, ^bDepartament de Química Física i Analítica, Universitat Jaume I (UJI), Castelló, Spain, ^cLaboratório de Bioquímica de Pequenas Moléculas, Departamento de Bioquímica, Escola Paulista de Medicina Unifesp, São Paulo, Brazil, ^dCentro de Pesquisa Leopoldo Américo Miguez de Mello CENPES/Petrobrás, Rio de Janeiro, Brazil, ^eCentro de Desenvolvimento de Materiais Funcionais, Departamento de Química, Universidade Federal de São Carlos, São Carlos, Brazil

Key Words

Carbon Nanotube • Nanoparticles • Cytotoxicity • Cellular viability • Oxidative stress • Apoptosis • Murine macrophages

Abstract

Background/Aims: The development of new nanomaterials has been growing in recent decades to bring benefits in several areas, especially carbon-based nanoparticles, which have unique physical-chemical properties and allow to take on several applications. Consequently, the use of new nanomaterials without previous toxicological studies raises concern about possible harmful health effects. The aim of this study was to investigate the cytotoxic profile of a new multi-walled carbon nanotube (MWCNT) functionalized with tetraethylenepentamine called OCNT-TEPA using *in vitro* assays in murine macrophage cells lineage J774 A.1. **Methods:** OCNT-TEPA was characterized by transmission electron microscopy (TEM) and high resolution TEM (HR-TEM), scanning electron microscopy (SEM), zeta potential and dynamic light scattering (DLS), and its cytotoxic effects were evaluated at 24 and 48 hours by cell viability assays (MTT and NR), morphology and cell recovery (optic microscopy and clonogenic assay), formation of reactive oxygen (ROS) and nitric oxide (NO) species, inflammatory profile (IL-6 and TNF cytokines), mitochondrial membrane potential analysis (MMP), activation of the caspase 3 pathway and cell death (flow cytometry). **Results:** The data showed a significant decrease in cell viability, increased production of ROS and NO, alteration of mitochondrial membrane potential, increased levels of inflammatory cytokines, alteration of cell morphology, activation

of the Caspase 3 pathway and consequently cell death, in the highest concentrations of OCNT-TEPA tested in the periods of 24 and 48 hours. **Conclusion:** The analyses showed that OCNT-TEPA has a dose-dependent cytotoxic profile, which may be harmful to murine macrophages (J774 A.1) and may represent a health risk.

© 2022 The Author(s). Published by
Cell Physiol Biochem Press GmbH&Co. KG

Introduction

Nanotechnology represents a very broad research area and is the latest and most advanced manufacturing technology on the rise worldwide. It is associated with the production of a variety of materials on a nanoscale by different chemical and physical methods. With dimensions below 100 nm, nanostructured materials have a growing interest in the field of nanotechnology and form the basis of this type of research. Nanomaterials allow access to various new options of magnetic, electronic, mechanical or optical properties. Nanotubes belong to a promising group of nanomaterials and currently carbon nanotubes (CNTs) represent the most important group [1, 2].

CNTs are a class of carbon allotropes with interesting properties, which makes their use relevant in several areas of nanotechnology [3]. Among its main chemical and physical properties, the high tensile strength, ultralight weight, special electronic structures and high chemical and thermal stability stand out. Due to these exceptional properties, scientists have developed an immense interest in these nanomaterials, which makes them the most widely explored carbon materials for various applications [1]. A CNT can be as thin as a few nanometers and as long as hundreds of microns. The structure, length, and number of layers vary in different shapes. Multi-walled carbon nanotubes (MWCNTs) consist of a collection of tubes with increasing diameters ranging from 3 to 30 nm [3].

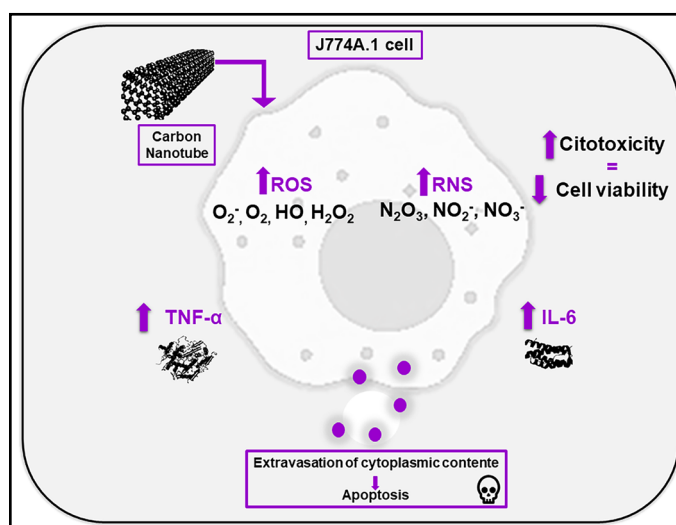
This study addresses the use of a carbon nanoparticle, called OCNT-TEPA. For its production, there was the insertion of a surface tetraethylenepentamine (TEPA) ligand after the nanoparticle was synthesized from an OCNT oxidized MWCNT. The insertion of this ligand allows the generation of a nanofluid with greater thermal stability, better viscosity, resistant to high temperatures and salinity. With this modification, it was possible to obtain more attractive characteristics when considering the application of this nanoparticle, since nanofluids are widely used in the oil and gas industry [4].

Today, nanotechnology impacts human life every day. In recent decades there has been the prosperous development and extensive applications of nanomaterials in many fields, including energy, aerospace, agriculture, industry, biomedicine and others [5]. The potential benefits are great and diverse, however, due to high human exposure to nanoparticles, there is significant concern about possible risks to health and the environment. These concerns led to the emergence of nanotoxicology, which is the study of the potential adverse effects of nanoparticles [6].

In this context, and based on the scarcity of studies with the nanoparticle OCNT-TEPA, a concern arises about the consequences that the modification of the carbon nanotube with the TEPA polymer can bring in terms of toxicity. It is necessary to evaluate possible undesirable effects, since this functionalization of the carbon nanotube can alter its surface area, conformation and physical-chemical properties. In view of this, it is important that the potential cytotoxic effects of OCNT-TEPA be evaluated in biological models. For this, this study elucidates the cytotoxic profile of OCNT-TEPA when exposed to a lineage of murine macrophages J774 A.1. Thus, it was possible to identify cellular damage by analyzing oxidative and inflammatory profiles, in addition to determining which metabolic mechanisms and pathways may be involved in these processes.

The representative scheme of the results delimited in this article is demonstrated in Fig. 1 at the moment when the OCNT-TEPA comes into contact with the J774 A.1 cell. Macrophages, in the presence of carbon nanotubes, activate defense systems generating an increase in the production of pro-inflammatory cytokines (IL-6 and TNF). The release of these cytokines can generate an inflammatory environment causing oxidative and nitrosative stress to cells,

Fig. 1. Effects triggered by exposure of OCNT-TEPA in Macrophages J774. A1.



which leads to the formation of reactive oxygen and nitric oxide species. In addition, the production of TNF is related to cell death by apoptosis, which also occurs with the presence of free radicals in the cell. The apoptosis process is also activated by the caspase pathway (Caspase 3) and any imbalance that occurs in the cell can generate membrane changes and cellular damage sufficient to reduce the viability of these cells in the presence of OCNT-TEPA.

Materials and Methods

Nanoparticle

The OCNT-TEPA sample was provided by Petrobras (Brazil). According to the manufacturer, the length of the particles varies between 2-10 μm and the diameter between 7 and 20 nm.

Characterizations

The samples were characterized by transmission electron microscopy (TEM) and high-resolution TEM (HR-TEM) using a Jeol 2100F microscope operating at 200 kV. The TEM sample was prepared by dripping an aqueous solution onto a carbon and copper grid, and dried at room temperature. Scanning electron microscopy (SEM) analyzes were performed using the Inspect F50 microscope operated at 5kV. The SEM sample was prepared by dropping an aqueous solution with the particles onto a silicon substrate. For the analysis of zeta potential and dynamic light scattering (DLS), the Malvern spectrometer Nano-ZS equipment was used.

Corona formation

Corona formation on the particles was evaluated through the increase in particle size obtained by DLS after incubation of the particles with the culture medium. First, the particles were incubated for 24 and 48 h with RPMI medium. These particles were centrifuged and DLS analysis was performed. After this analysis, the same particles were washed three times in distilled water and the DLS analysis was performed again.

Cell culture

The cell line of murine macrophages J774 A.1 (code 0121) obtained from Rio de Janeiro Cell Bank (BCRJ) was cultivated in RPMI medium (Roswell Park Memorial Institute Medium, Sigma-Aldrich, USA) supplemented with 10% fetal bovine serum (SFB, LGC Biotechnology) and incubated at 37 °C and 5% CO_2 . The tests were performed with the following concentrations of OCNT-TEPA: 1, 50, 250, 500 and 1000 $\mu\text{g/ml}$ for 24 and 48 hours.

Determination of OCNT-TEPA concentrations, MTT cytotoxicity assay, neutral red dye (VN) and EC₅₀ determination

The cytotoxicity of OCNT-TEPA was evaluated by the colorimetric assay with MTT salt and with the dye VN (Neutral Red) independently. MTT salt [3-(4,5-dimethylthiazol-2-yl) 2,5-diphenyltetrazolium bromide] – Sigma-Aldrich, USA) assesses the integrity of mitochondrial function through the formation of formazan crystals, the higher the crystal production, the greater the cell viability [7]. The VN (Scientific Exodo) assay is based on dye® accumulation in lysosome membranes, the more viable cells, the greater the diffusion of the dye by the membrane [8].

Initially, the MTT assay was applied to determine which concentration would be tested based on the literature that reported that the concentrations of nanoparticles most commonly tested ranged from 1 to 1000 µg/ml [9, 10]. The selection criteria was to use the most toxic and non-toxic concentrations (1, 10, 50, 100, 250, 500, 750 and 1000 µg/ml) between the concentrations initially tested. Concentrations of 1, 50, 250, 500 and 1000 µg/ml were selected to perform the study.

In a plate of 96 wells 1×10⁴ cells/well were seeded and exposed to different concentrations of OCNT-TEPA. After 24 and 48 hours of exposure the wells were washed with PBS 1X (saline phosphate buffer) and 100 µl of MTT solution (0, 5 mg/ml in PBS 1X plus incomplete RPMI medium and without phenol [1:5]) and 100 µl of VN dye (30 µg/ml in DMEM medium supplemented with 1% SBF and without phenol) were added and the reaction occurred for 4 hours (MTT) and 2 hours (VN) at 37 °C and 5% CO₂. The formazan crystals were solubilized with 100 µl of DMSO (MTT) and for the VN 200 µl test of the diluent containing 50% ethanol and acetic acid 1% (1:1 1) were added and the reading was performed at 570 nm (MTT) and 540 nm (VN) in a plate spectrophotometer (Thermo Scientific™ Multiskan™ GO Microplate Spectrophotometer). The MTT absorbance data were used to calculate EC₅₀ (concentration that induces half of the maximum effect). The percentage of cell viability (MTT and VN) was calculated by comparing the values obtained with the control mean according to equation 1:

$$\% \text{ cytotoxicity} = \frac{\text{Experimental Group} \times 100}{\text{CTRL group SD}}$$

Cellular morphology by optical microscopy

For the analysis of cell morphology in a plate of 96 wells, 1×10⁴ cells per well were seeded and exposed to different concentrations of OCNT-TEPA. After 24 and 48 hours of exposure, the wells were washed with PBS 1X and the morphology was observed in an Optical Microscope Axiovert 40 CFL (Zeiss), with objective lens 10X, which images were captured with the camera coupled model LOD-3000 (Bio Focus) and analyzed by future winjoetm software version 2.0 in final resolution of 100X.

Detection of reactive nitrogen species (RNS)

The detection of RNS was made through the Griess Reaction, which assess the indirect production of nitric oxide (ON) by the production of nitrate ion (NO₂) [11, 12]. In a plate of 96 wells were seeded 1×10⁴ cells/well and exposed to different concentrations of OCNT-TEPA. After exposure time of 24 and 48 hours, 50 µl of antinatat was collected and transferred to a new 96-well plate, followed by the addition of 50 µl of Griess solution (1:1 mixture of solution A [1% sulfanilamide in 5% phosphoric acid] and solution B [0.1N-1-naphthylein diamine]) at room temperature for 15 minutes. Absorbance was read at 554 nm with plate spectrophotometer (Thermo Scientific™ Multiskan™ GO Microplate Spectrophotometer). The nitrite concentration in the supernatant is quantified using the standard curve provided in the kit and the nitrite concentration is shown in mM.

Detection of reactive oxygen species (ROS)

The detection of ROS production was performed using the DCFH-DA fluorescent probe (2',7'-Dichlorodihydrofluorescein Diacetate, Sigma-Aldrich, USA). In a plate of 96 wells, 1×10⁴ cells/well were seeded and exposed to different concentrations of OCNT-TEPA. After exposure of 24 and 48 hours, the medium was removed, and the DCFH-DA probe (100 mM) was solubilized in RPMI medium without FBS and without phenol and was added to each well; the reaction occurred for 30 minutes at 37 °C and 5% OF CO₂ protected from light. Then the wells were washed with PBS 1X. Fluorescence emission reading was measured at 485-530 nm in spectrophotometer of Spectra MAX I3 VR (Molecular Devices) plates. The percentage of cell viability was calculated using equation 1.

Cell recovery

The cell recovery capacity after the proposed treatment was evaluated by the clonogenic assay, which analyzes the ability of cells to recover through colony formation [13]. In a plate of 6 wells were seeded 1×10^3 cells per well and exposed to different concentrations of OCNT-TEPA. After exposure of 24 and 48 hours, the wells had the medium discarded, were washed with PBS 1X and new culture medium was added. After 7 days of recovery, with 2 changes of medium, the cells were fixed with methyl alcohol P.A. (absolute methanol) and dyed with 0.1% violet crystal (diluted in distilled water). The wells were photographed and the colony count performed in the Software ImageJ version 1.53^a. Colony count was also performed by dilution of colonies with SDS 1% (sodium dodecyl sulfate). Absorbance was read at 570 nm in plate spectrophotometer (Thermo Scientific™ Multiskan™ GO Microplate Spectrophotometer).

Detection of IL-6 and TNF

IL-6 and TNF cytokine levels were measured using the ELISA quantification kit following manufacturer's standards (BD Biosciences). In a plate of 24 wells, 5×10^5 cells/well were seeded and exposed to different concentrations of OCNT-TEPA for 24 and 48 hours. After the exposure period, the supernatant was collected and 50 μ l from the pool were added to a 96-well ELISA plate, already sensitized with capture antibodies and blocked with 0% fat milk proteins. Then, the secondary antibody conjugated with the enzyme peroxidase was added. After 2 hours, the enzymatic substrate TMB (3,3',5,5'-Tetramethylbenzidine) was added to the wells revealing the reaction. The absorbance reading was measured at 450 nm in a plate spectrophotometer (Thermo Scientific™ Multiskan™ GO Microplate Spectrophotometer) and the concentrations were calculated from a standard curve for each sample provided by the kit.

Mitochondrial membrane potential analysis

Rhodamine 123 is a fluorochrome specific to mitochondrial marking in living cells. Because it is a cationic fluorochrome is attracted by the high negative electrical potential of the mitochondrial membrane, incorporating itself inside these organelles, presenting green fluorescence. Changes in the level of mitochondrial integrity can be detected by increased cytosolic green fluorescence, indicating a diffusion of Rhodamine 123 from mitochondria to the cytosol [14]. In a plate of 24 wells, 1×10^5 cells/well were seeded and exposed to different concentrations of OCNT-TEPA for 24 and 48 hours. After exposure times, the plates were centrifuged and washed with PBS 1X and 100 μ l/well of Rhodamine 123 antibody (5 mg/ml diluted in ethanol) were added. The reaction occurred for 30 minutes at 37 °C, with 5% CO₂ and protected from light. Then, the cells were removed with the aid of a scraper and resuspended in 300 μ l of PBS 1X. The reading was performed in a Flow Cytometer Accuri™ C6 BD Biosciences) with 10,000 events using FlowJo™ version X software (BD Biosciences).

Caspase 3 levels dosage

For the detection of apoptosis via increased caspase-3 activity, the EnzChek® Caspase-3 Assay Kit #1 was sown 1×10^5 cells/well and exposed to different concentrations of OCNT-TEPA for 24 and 48 hours. After the exposure period, the plaque was centrifuged and the cells were removed with the aid of a scraper and PBS 1X. Cell extract was lysed with lysis buffer for 30 minutes at -20 °C and centrifuged at 5000 g for 5 minutes. Then, 50 μ l of the supernatant was added to 50 μ l of the reagent solution (Z-DEVD-AMC in reaction buffer) in a 96-well plate. The reaction occurred for 30 minutes at room temperature. Fluorescence emission was read at 342 - 441 nm in Spectra MAX i3™ (Molecular Devices) equipment.

Cell death by apoptosis

Cell death by apoptosis was identified by means of the Annexin V PE and 7AAD marker detection kit (BD Biosciences). In a plate of 24 wells, 1×10^5 cells/well were seeded and exposed to different concentrations of OCNT-TEPA for 24 and 48 hours. After the exposure period, the plates were centrifuged at 1500 rpm at 4 °C, washed with PBS 1X and the antibodies PE Annexin V and 7AAD [1:1] (1 ml/well in 1:10 binding buffer) were added. The reaction occurred for 15 minutes at room temperature protected from light. Subsequently, the cells were removed with the aid of a scraper and resuspended in microtubes with 300 μ l of binding buffer. The analyses were performed in a flow cytometer (Accuri™ C6 BD Biosciences) with 10,000 events per gate, using FlowJo™ version X (BD Biosciences) software.

Statistical analyses

The data obtained in this study were expressed on \pm SD and analyzed using GraphPad Prism 7.0 (San Diego, California, USA) and sigmaplot software (version 14). The entire study was carried out in at least two biological triplicates and in two independent experiments. The data were analyzed by the Shapiro-Wilk test, analysis of variance by the Brown-Forsythe test followed by the analysis with One Way RM ANOVA to verify the parametric or non-parametric nature of the data. For this, the ANOVA test (variance analysis) was applied to parametric data and the Tukey multiple comparison scan (the results were presented in mean and standard deviation). For nonparametric data, the Kruskal-Wallis test and Dunn's multiple comparison post-test were used (the results were presented as the median with the upper and lower quartiles: Me [Q1; Q3]). Statistical significance was established at $p < 0.05$.

Results

Through Fig. 2A it is possible to observe in the SEM images a good uniformity in the morphologies of the OCNT-TEPA sample. From the TEM image of Fig. 2B, a small dispersion of the internal diameter of the sample is observed, obtaining an average value of 12.9 ± 4.7 nm (Fig. 2D). The OCNT-TEPA was observed in details through HR-TEM images (Fig. 2C), obtaining an average internal diameter value of 4.9 ± 1.8 nm (Fig. 2E). Experimentally, it is difficult to estimate the average length of the particles, since the tangle of nanotubes ends up overlapping one on the other. However, according to the manufacturer, the length varies between 2 and 10 μ m. The zeta potential values for the particles in the water and in the culture, medium was -6.74 ± 1.21 and -4.93 ± 0.82 mV, respectively. These slightly negative values are related to the presence of carboxylic groups on the surface of the sample, in addition this small decrease in the zeta potential values may be related to the formation of corona in the samples, which can lead to their aggregation. To confirm the formation of corona on the surfaces of the particles, the sample was incubated with the culture medium for 24 and 48 hours, and their size was analyzed using DLS technique (Fig. 2F).

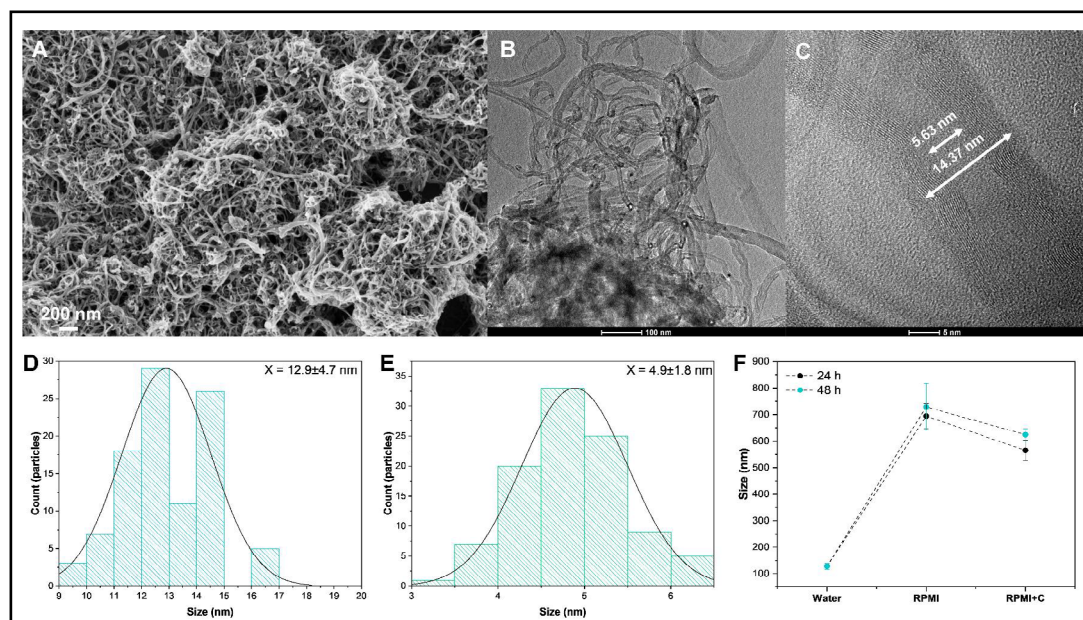


Fig. 2. (A) SEM, (B) TEM, and (C) HR-TEM images of the OCNT-TEPA sample. (D) Length and (E) Width size distribution of the nanoparticles. (F) Particle size variation obtained by DLS after incubation (24 and 48 hours) with the culture medium (RPMI) and after washing with distilled water (RPMI+C).

For the sample in water, the value obtained was 128 ± 11 nm, showing that the even dispersed material presents an aggregation rate. After 24 and 48 hours of incubation with the culture medium, a large increase in DLS values is observed, increasing to 694 ± 48 and 729 ± 88 nm, respectively. Furthermore, after washing with water, the size remains much larger than the initial size in water, obtaining values of 565 ± 38 and 624 ± 22 nm. This high stability size increases the evidence of the sample particles aggregation due to the formation of corona, which agrees with the results obtained in previous work [15]. This excessive aggregation due to corona formation can significantly alter the physicochemical properties of the particles, in addition to altering their behavior in a biological environment [16].

Fig. 3 shows cell viability in % of different concentrations of OCNT-TEPA in macrophages J774 A.1 after 24 and 48 hours exposure periods. Analyzes performed using the MTT assay showed a significant decrease in cell viability when exposed to 50, 250, 500 and 1000 $\mu\text{g}/\text{ml}$ of OCNT-TEPA in a 24 hours period compared with the control group. Within 48 hours of exposure, there was also a decrease in viability for concentrations of 250, 500 and 1000 $\mu\text{g}/\text{ml}$ of OCNT-TEPA (Fig. 3A). EC50 was calculated for each concentration and exposure time (24 and 48 hours) and the results were EC50 24.84 at 24 hours and EC50 30.44 at 48 hours of exposure (Fig. 3B). Data using VN assay (Fig. 3C) resulted in a significant reduction in cell viability at concentrations of 250, 500 and 1000 $\mu\text{g}/\text{ml}$ of OCNT-TEPA in the periods of 24 and 48 hours of exposure when compared with the control group showing possible OCNT-TEPA cytotoxicity in macrophages J774 A.1 from a concentration of 250 $\mu\text{g}/\text{ml}$.

The colony formation test (clonogenic assay) of Fig. 4 showed a significant decrease in the number of colonies formed (qualitative data), when exposed to concentrations of 250, 500 and 1000 $\mu\text{g}/\text{ml}$ of OCNT-TEPA in the intervals of 24 and 48 hours compared to the control (Fig.4A and B). The data to Fig. 4C indicates the quantification of these colonies by absorbance reading, after detachment of the colonies from the plates, which showed a significant decrease in the concentrations of 250, 500 and 1000 $\mu\text{g}/\text{ml}$ of OCNT-TEPA for 24 and 48 hours (quantitative data), showing similar results to the analysis of the number of colonies. As a non-colorimetric test, the clonogenic assay allows us to certify all of our viability tests.

The cellular morphology of macrophages J774 A.1 after periods of 24 and 48 hours of exposure to OCNT-TEPA at different concentrations (1, 50, 250, 500 and 1000 $\mu\text{g}/\text{ml}$ and control group) is demonstrated through qualitative data in Fig. 5. The images showed changes in the cell structure when in contact with the highest concentrations of OCNT-TEPA (250, 500 and 1000 $\mu\text{g}/\text{ml}$), visibly registering a reduce number of cells in the two analyzed periods in relation to the control. These results corroborate the tests applied to cell viability, because at the highest concentrations tested, we observed few intact cells, with probable occurrence of cell lysis.

Fig. 3. Cellular viability of J774. A1 on exposure to OCNT-TEPA. Data sampled by (A) MTT, (B) EC50 and (C) NR in the periods of 24 and 48 hours of exposure. (*) vs. Control in 24 hours; * $p < 0.05$; ** $p < 0.01$; p < 0.001 ; p < 0.0001 . (#) vs. Control in 48 hours; # $p < 0.05$; ## $p < 0.01$; ### $p < 0.001$; #### $p < 0.0001$.

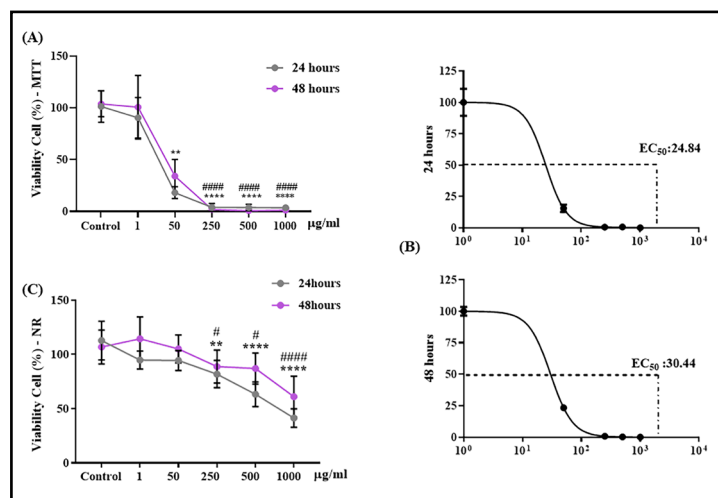


Fig. 4. Formation of J774 A.1 colonies on exposure to OCNT-TEPA. Data sampled by (A) Colonies of cells formed after 7 days of recovery, (B) Number of colonies formed, (C) Quantification of absorbance of recovered colonies, in the periods of 24 and 48 hours of exposure. (*) vs. Control in 24 hours; * p <0.05; ** p<0.01; p <0,001; # p <0.0001. (#) vs. Control in 48 hours; # p <0.05; ## p<0.01; ### p <0,001; #### p<0.0001.

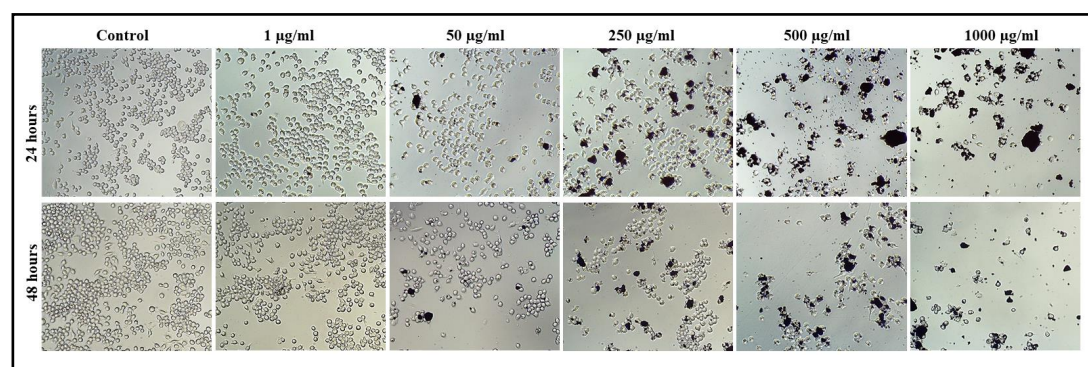
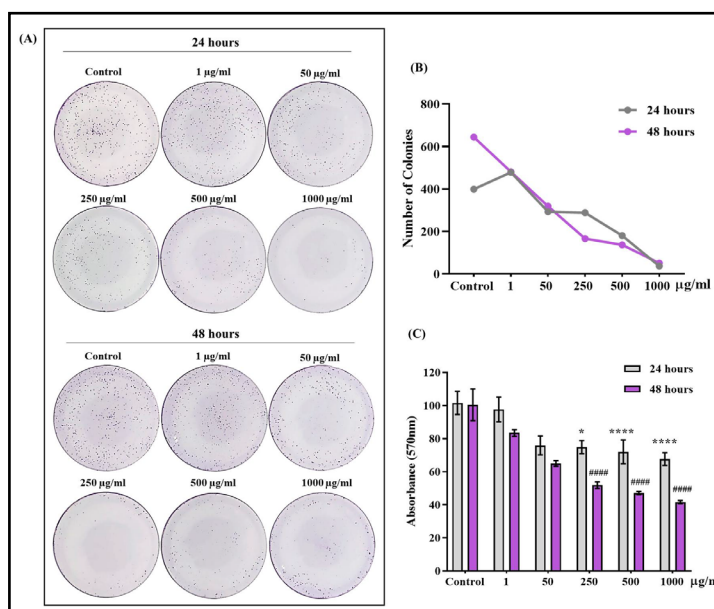


Fig. 5. Cellular Morphology of J774 A.1 on exposure to OCNT-TEPA. Cell morphology is represented by optical microscopy images with a total increase of 100X in the control groups and exposed to concentrations of 1, 50, 250, 500 and 1000 µg/ml of OCNT-TEPA for 24 and 48 hours.

Fig. 6 relates the oxidative stress (ROS) and nitrosative (RNS) pathway and the inflammatory profile through the cytokines IL-6 and TNF. Fig. 6 shows the ability of different concentrations of OCNT-TEPA to induce the formation of intracellular reactive oxygen species (ROS) in macrophages J774 A.1 using DCF-DA fluorescence as an inducer of intracellular oxidant production. The periods of 24 and 48 hours of exposure showed a significant increase in ROS production at concentrations of 250, 500 and 1000 µg/ml of OCNT-TEPA when compared to the control group. Fig. 6B shows the analysis of nitrosative stress through the production of nitric oxide (NO) by the Griess reaction in macrophages J774 A.1 cells when exposed to OCNT-TEPA concentrations for 24 and 48 hours. There was a significant increase in 24 hours of exposure for the concentration of 1000 µg/ml and in the period of 48 hours the increase occurred for the concentrations of 500 and 1000 µg/ml of OCNT-TEPA. These ROS and RNS production data at the highest concentrations of the nanoparticle demonstrate the presence of free radicals being formed in macrophages J774 A.1. Fig. 6C and 6D show quantification data for IL-6 and TNF cytokines, respectively. The production of IL-6 in macrophages J774 A.1 showed a significant increase at concentrations of 250, 500 and 1000 µg/ml of OCNT-TEPA in the periods of 24 and 48 hours, while the production of TNF had significant changes in the two periods at concentrations of 500 and 1000 µg/ml when compared to the control group, demonstrating a possible inflammatory response in the presence of the highest concentrations of OCNT-TEPA.

Fig. 6. Analysis of ROS, RNS, IL-6 and TNF in J774 A.1 when exposed to OCNT-TEPA. (A) ROS production in %; (B) PRODUCTION of RNS in %; (C) IL-6 cytokine production; (D) TNF cytokine production. All data analyzed in 24 and 48 hours of exposure. (*) vs. Control in 24 hours; * p <0.05; ** p <0.01; p <0,001; p <0.0001. (#) vs. Control in 48 hours; # p <0.05; ## p <0.01; ### p <0,001; #### p < 0.0001.

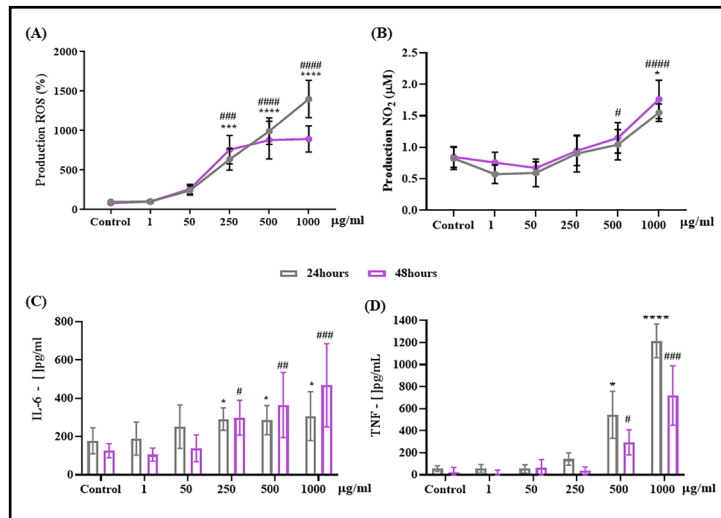
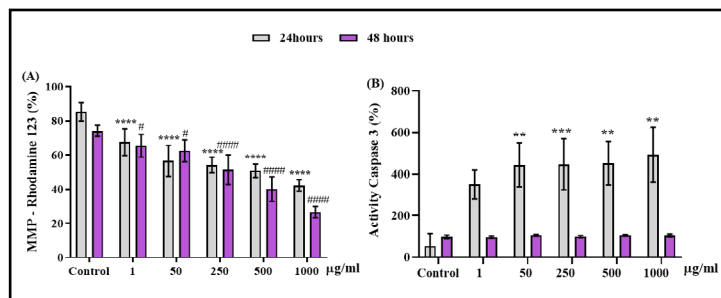


Fig. 7. Evaluation of mitochondrial membrane potential (MMP) and Activation of Caspase3 in J774 A.1 exposed to OCNT-TEPA. (A) Quantification of Rhodamine 123(%) to evaluate MMP; (B) Production of Active Caspase 3. Data presented in periods of 24 and 48 hours of exposure to OCNT-TEPA. (*) vs. Control in 24 hours; * p <0.05; ** p <0.01; p <0,001; p <0.0001. (#) vs. Control in 48 hours; # p <0.05; ## p <0.01; ### p <0,001; #### p <0.0001.



The cellular alterations caused by the exposure of OCNT-TEPA at different concentrations (1, 50, 250, 500 and 1000 µg/ml) and control are demonstrated in Fig. 7 by evaluation methods of Rhodamine123 and Caspase 3. Changes in mitochondrial membrane potential (MMP) were detected by analysis of Rhodamine 123 fluorescence in macrophages J774 A.1 at 24 and 48 hours of exposure to OCNT-TEPA, at concentrations of 1, 50, 250, 500 and 1000 µg/ml (Fig. 7A) suggesting possible damage to the mitochondrial membrane of cells. Caspase 3 is responsible for clogging and initiating the degradation of various cellular proteins. The activation of Caspase 3 is demonstrated in Fig. 7B only in the period of 24 hours of OCNT-TEPA exposure, highlighting a significant increase in concentrations of 50, 250, 500 and 1000 µg/ml in relation to the control. The 48 hours display interval of OCNT-TEPA showed no significant data on Caspase 3 production when compared to the control group.

Cell death pathway analyzes were performed by flow cytometry and illustrated by Dot Plot graphs (Fig. 8). Expressed as % cellular fluorescence, the 7AAD marker was used to detect late apoptosis/necrosis and Annexin V/PE to mark cells in initial apoptosis after exposure to OCNT-TEPA from J774 A.1 macrophages for 24 and 48 hours. 7AAD is demonstrated in quadrant Q1 (late apoptotic/necrotic cells), Annexin V/PE demonstrated in quadrant Q2/Q3 (initial apoptotic cells) and living cells demonstrated in quadrant Q4 (Fig. 8A). The histograms are demonstrated by fluorescence peaks of both markers according to each concentration of OCNT-TEPA analyzed (Fig. 8B). For the 24 hours period of exposure, there is a progressive increase for both initial apoptosis and late apoptosis/necrosis according to the increase in concentrations tested, the higher the concentration of OCNT-TEPA, the higher the fluorescence peak of these markers. Data obtained at 48 hours of exposure showed peaks of

initial apoptosis up to the concentration of 250 $\mu\text{g/ml}$ and higher peaks of late apoptosis/necrosis for concentrations of 500 and 1000 $\mu\text{g/ml}$.

The graphs of Fig. 9 show that in the 24 hours period there was a significant increase in initial apoptotic cells in concentrations from 50 $\mu\text{g/ml}$ of OCNT-TEPA in relation to the control. In 48 hours of exposure, only concentrations of 50 and 250 $\mu\text{g/ml}$ presented significant initial apoptosis (Fig. 9A). In relation to late apoptotic cells/necrosis, there was a significant increase in groups 50, 250, 500 and 1000 $\mu\text{g/ml}$ of OCNT-TEPA in 24 hours and 250, 500 and 1000 $\mu\text{g/ml}$ in 48 hours (Fig. 9D), when compared with the control group. These data detail the results presented in the fluorescence peak analyzes for the markers (Fig. 8B).

In Fig. 9B and 9C the heatmap graphs are demonstrated, presenting the correlation in the mean amount of initial and late apoptotic cells/necrosis, in 24 and 48 hours of exposure to OCNT-TEPA, at concentrations of 1, 50, 250, 500 and 1000 $\mu\text{g/ml}$ using the cell line macrophages J774A.1. The green color represents the minimum value and the red value obtained from the average number of cells.

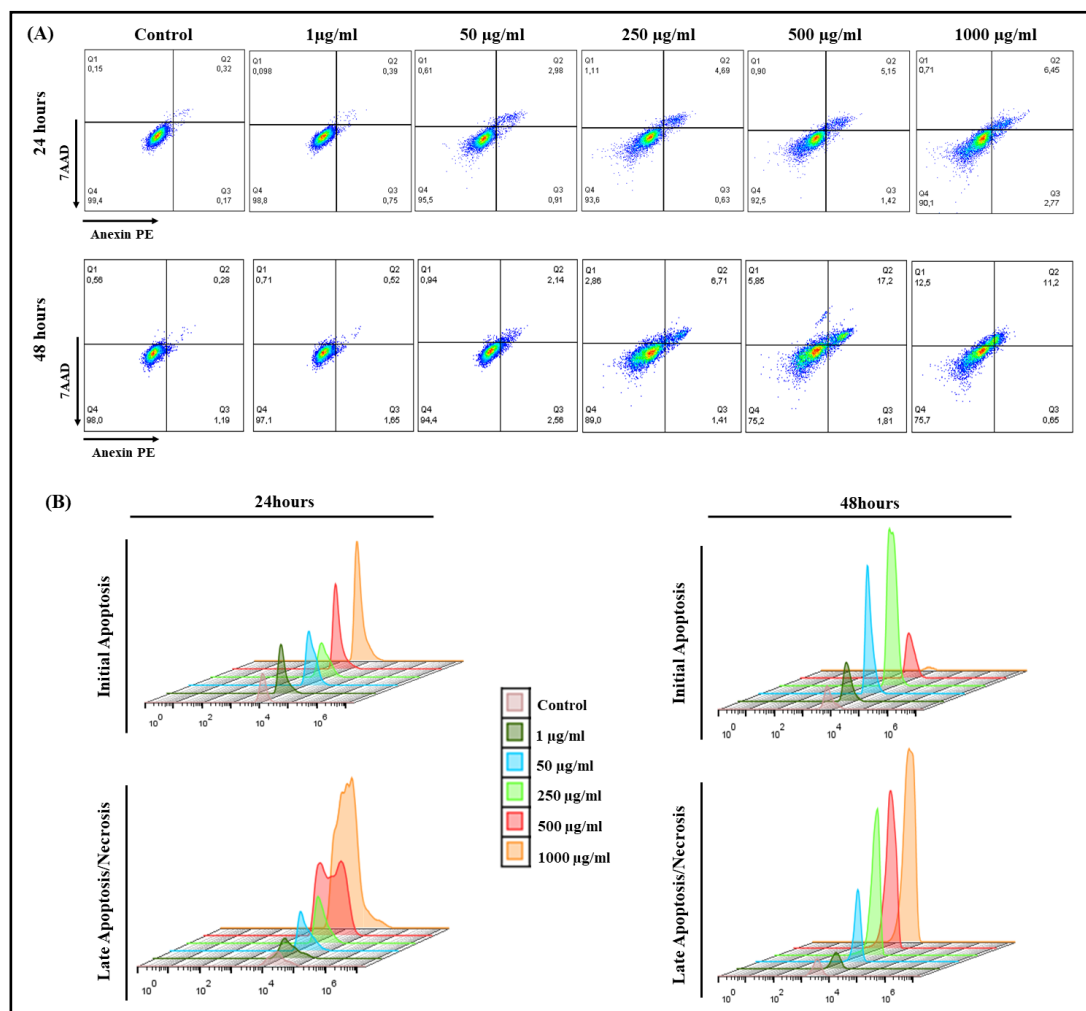


Fig. 8. Analysis of cell death in J774 A.1 exposed to OCNT-TEPA with PE annexin V and 7AAD markers. (A) Histograms of each concentration in 24 and 48 hours. (B) Fluorescence emission peak charts for initial and late apoptosis/necrosis.

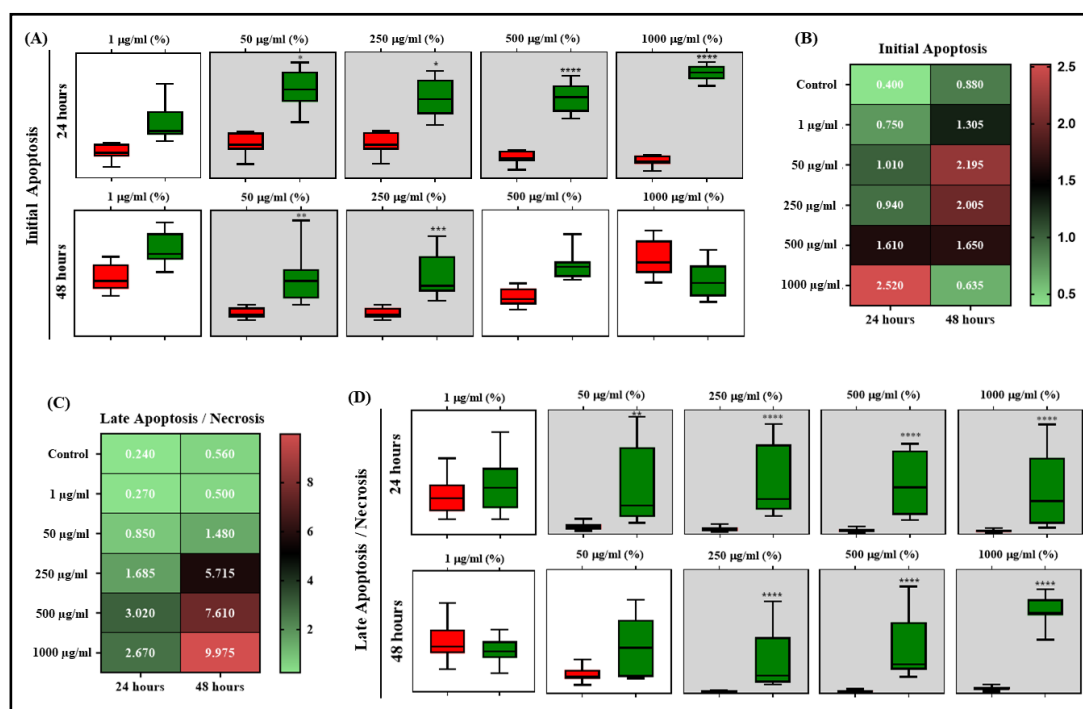


Fig. 9. Analysis of cell death in J774 A.1 exposed to OCNT-TEPA. (A) Initial apoptosis in % of each concentration in relation to the control for 24 and 48 hours of exposure to OCNT-TEPA. The gray background represents a significant difference. (B) Correlation of the periods of 24 and 48 hours for initial apoptosis. (C) Correlation of 24 and 48 hours periods for late apoptosis/necrosis. (D) Late apoptosis/necrosis in % of each concentration in relation to the control for 24 and 48 hours of exposure to OCNT-TEPA. The gray background represents a significant difference. (*) vs. Control in 24 hours; * $p < 0.05$; ** $p < 0.01$; # $p < 0.001$; #> $p < 0.0001$. (#) vs. Control in 48 hours; # $p < 0.05$; ## $p < 0.01$; ### $p < 0.001$; #### $p < 0.0001$.

Discussion

The widespread and frequent use of carbon nanomaterials, which make up from industry to medicine and biotechnology, currently raises concerns about health risks when exposed to the properties of these materials [17, 18]. These issues make it increasingly important to develop research to assess the potential toxic effects of nanomaterials before their spread through the environment [17].

The cellular mechanisms of nanomaterial-induced cytotoxicity are being evaluated preferably by assays using *in vitro* models, as they offer greater control over the experimental variables that occur most frequently in *in vivo* assays. Carbon nanoparticles are studied in several cell types, with emphasis on macrophages, which are the most used cells because they present as the first line of defense of the immune system [17]. Thus, in this study, we used the macrophage lineage of murine J774 A.1 to perform cytotoxicity tests in the presence of a functionalized multi-chain carbon nanotube (MWCNT) called OCNT-TEPA.

Several studies using carbon-based nanomaterials have shown some cytotoxic effects, including increased ROS production, damage to genetic material, alteration of mitochondrial activity and cell death [19]. The same was observed in the present study in relation to cell viability analyses using Neutral MTT and Red assays for macrophages J774 A.1 exposed to various concentrations of OCNT-TEPA for periods of 24 and 48 hours. There was a significant reduction in the viability of J774 A.1 in the highest concentrations of OCNT TEPA tested, indicating possible cytotoxic effects dependent on mitochondrial enzymes, since there was a decrease in MTT metabolism in cells. Neutral red has the same purpose, but is able to be

absorbed by living cells and concentrate inside lysosomes for quantification of living cells [20, 21]. These data corroborate other experiments carried out with MWCNTs using lines of murine alveolar macrophages (MH-S) and murine peritoneal macrophages (raw264.7), which showed decreased cell viability in the presence of higher concentrations of MWCNTs [22]. Nahle et al. also observed CNT cytotoxicity using rat alveolar macrophages (NR8383) in cell viability experiments [23].

Cell proliferation analyses through colony formation and microscopy of the morphology of J774 A.1 confirm the results of cellular viability, since the clonogenic assay analyzes the long-term recovery capacity of cells after exposure, being considered an useful tool among cytotoxicity tests by CNTs. Louro et al. analyzed the decrease in the proliferation of different cell lines when exposed to several MWCNTs [24]. Cell morphology images also visibly show a decrease in the number of cells in the highest concentrations of OCNT-TEPA. These results corroborate studies that used the same OCNT-TEPA nanoparticle in murine fibroblast cells (LA-9) [15].

Several studies suggest that the contact of nanoparticles with the cellular environment of macrophages may alter the mechanism of absorption of these cells, such as the presence of long-chain CNTs, which can induce unsuccessful phagocytosis in macrophages, generating inflammatory response, increased production of cytokines and ROS [17, 25, 26]. In this study, the generation of reactive oxygen and nitrogen (ROS/RNS) species in 24 and 48 hours of exposure to OCNT-TEPA was also evaluated to analyze oxidative/nitric stress in J774 A1. The results showed a significant increase in nitric oxide (NO) and ROS production in the two periods tested, but the ROS production in 24 h was even higher when compared to the results in 48 hours of exposure. The ROS quantification data corroborate the findings by Sabido et al., who tested CNTs in RAW murine macrophages and observed an increase in ROS production initially and subsequently decrease in the production of this compound after exposure for longer periods of CNTs, characterizing oxidative stress as a rapid and transitory process [27]. Oxidative stress has the ability to trigger and maintain inflammation mechanisms, generating possible toxic effects on cells, as well as overproduction of ROS can act directly on biological structures causing damage to cellular functions [27–29].

The induction of oxidative stress in J774 A.1 cells may be related to the presence of inflammatory cytokines, since the increase in the level of TNF in cells favors the production of IL-6, contributing to cell death [30, 31]. The analyses indicated an increase in the production of IL-6 and TNF in J774 A.1 in the presence of OCNT-TEPA in 24 and 48 hours, as well as the data obtained by Zhang et al., which showed significant production of TNF and IL-6 in RAW 264.7 macrophages, in the presence of functionalized MWCNTs [17, 32]. In general, IL-6 is present in various stages of inflammation and can activate ROS pathways through active oxygen metabolites that will be formed after the production of TNF. All these steps lead to the activation of the cellular apoptosis pathways [31, 33].

The effects of OCNT-TEPA in J774 A.1 were also investigated in relation to mitochondrial activity, which is responsible for cell viability and proliferation by evaluating mitochondrial membrane potential (MMP), characterized by regulating mitochondrial functions. Changes in macrophage membrane potential were observed when exposed to OCNT-TEPA for 24 and 48 hours from the quantification of Rhodamine 123 (Rh123) present in the samples. These alterations may also evidence subsequent signaling for cellular apoptosis [34, 35].

Visalli et al. analyzed the MMP of human lung cells when exposed to CNTs and observed a drop in Rh123 quantification in the period of 1 to 7 days of exposure. Several studies have reported that CNTs may alter mitochondrial membrane potential through exaggerated ROS formation, cytochrome C release, and changes in mitochondrial electron chain complexes [29, 34, 36, 37]. In addition, the release of cytochrome C from the inside of the mitochondrial membrane triggers a pathway of cellular apoptosis by activating the Caspases pathway [34, 38].

The Caspases pathway is formed by a set of proteases that are activated one by one during apoptotic signaling [39, 40]. Initially, caspases called initiators (caspases 8, 9 and 10) are activated, which will later activate effector caspases (caspases 3, 6 and 7), responsible

for the degradation of proteins important for homeostasis and cellular function, causing the death of target cells [40–43]. The activation of caspase 3 was analyzed after exposure to OCNT-TEPA in macrophages J774 A.1 and the result demonstrated induction of caspase 3 only within 24 hours of exposure, suggesting caspase-induced apoptosis 3 under these conditions. At the end of 48 hours of exposure to OCNT-TEPA there was no activation of caspase 3 and consequently the apoptosis pathway was not activated. The comparison of the different parameters obtained between the periods of 24 and 48 hours in this assay may suggest that in longer exposure periods there is an increase in the damage caused in the cell membrane. These damages can cause the activation of the signaling cascade that favors cell death by necrosis [44].

Data from cell death analyses of the present study contribute to a better understanding of the results discussed to date, since experiments using apoptosis markers reveal that exposure of the nanoparticle OCNT-TEPA in 24 and 48 hours resulted in apoptosis of macrophages J774 A.1. This result presents the same pattern of cell death analyses performed with MWCNT OCNT-TEPA in murine fibroblast cells (LA-9), which demonstrated incidence of initial apoptosis at the first moment (24 hours of exposure), progressing to late apoptosis or possible cellular necrosis in longer periods of exposure, or higher concentrations of OCNT-TEPA, due to the fact that these concentrations present nanoparticle aggregates that can alter mechanisms of cell death through membrane damage [15, 45].

Conclusion

In general, the results presented in this study suggest a potential cytotoxic effect of OCNT-TEPA for the macrophage cell line J774 A.1 that depends on the dose and time of exposure. The analyses showed that concentrations of this nanoparticle generate possible cell death of J774 A.1 because of several factors such as high production of cellular oxidative stress, possible damage to the mitochondrial membrane, inflammatory profile and activation of the caspases 3 for the purpose of apoptotic signaling, causing a decrease in cell viability. Given these data, the importance of research that addresses the toxicity of nanoparticles before the mass use of these nanomaterials in whatever application is indisputable.

Acknowledgements

The authors would like to thank Dra. Márcia Regina Cominetti (Departamento de Gerontologia, Universidade Federal de São Carlos, São Carlos, SP, Brazil) for availability of equipment.

Author Contributions

Study development: Krissia, Joice, Bruna.

Study design: Carlos, Fernanda.

Data analysis: Krissia, Joice, Bruna, Marcelo.

Preparation of the article: Krissia, Joice, Bruna, Luciana, Camila, Patricia, Marcelo.

Contribution of equipment and analysis: Elson, Marcelo.

Funding

This study was supported by PETROBRAS/Project: Proc. No 2017/00010-7. M.A. was supported by the Margarita Salas postdoctoral contract MGS/2021/21 (UP2021-021) financed by the European Union – Next Generation EU. The authors would also like to thank the financial aid from the Fundação de Amparo à Pesquisa do Estado de São Paulo – FAPESP (2013/07296-2), the Financiadora de Estudos e Projetos – FINEP, the Coordenação de Aperfeiçoamento de Pessoal de Nível Superior – CAPES (Financial Code 001) and the Conselho Nacional de Desenvolvimento Científico e Tecnológico – CNPq.

Disclosure Statement

The authors have no conflicts of interest to declare.

References

- 1 Anzar N, Hasan R, Tyagi M, Yadav N, Narang J: Carbon nanotube - A review on Synthesis, Properties and plethora of applications in the field of biomedical science. *Sensors International* 2020; DOI: 10.1016/j.sintl.2020.100003.
- 2 Kumar S, Rani R, Dilbaghi N, Tankeshwar K, Kim KH: Carbon nanotubes: A novel material for multifaceted applications in human healthcare. *Chem Soc Rev* 2017;46:158-196.
- 3 Mohanta D, Patnaik S, Sood S, Das N: Carbon nanotubes: Evaluation of toxicity at biointerfaces. *J Pharm Anal* 2019;9:293-300.
- 4 Lima MCF, Amparo SZS do, Siqueira EJ, Miquita DR, Caliman V, Silva GG: Polyacrylamide copolymer/aminated carbon nanotube-based aqueous nanofluids for application in high temperature and salinity. *J Appl Polym Sci* 2018; DOI: 10.1002/app.46382.
- 5 Liu Y, Zhu S, Gu Z, Chen C, Zhao Y: Toxicity of manufactured nanomaterials. *Particuology*. 2022;69:31-48.
- 6 Hulla JE, Sahu SC, Hayes AW: Nanotechnology: History and future. *Hum Exp Toxicol* 2015;34:1318-1321.
- 7 Mosmann T: Rapid Colorimetric Assay for Cellular Growth and Survival: Application to Proliferation and Cytotoxicity Assays. *J Immunol Methods* 1983;65:55-63.
- 8 Repetto G, del Peso A, Zurita JL: Neutral red uptake assay for the estimation of cell viability/ cytotoxicity. *Nat Protoc* 2008;3:1125-1131.
- 9 Du J, Wang S, You H, Zhao X: Understanding the toxicity of carbon nanotubes in the environment is crucial to the control of nanomaterials in producing and processing and the assessment of health risk for human: A review. *Environ Toxicol Pharmacol* 2013;36:451-462.
- 10 Kinaret PAS, Scala G, Federico A, Sund J, Greco D: Carbon Nanomaterials Promote M1/M2 Macrophage Activation. *Small* 2020;16:1907609.
- 11 Green LC, Wagner DA, Glogowski J, Skipper PL, Wishnok JS, Tannenbaum SR: Analysis of Nitrate, Nitrite, and [15N]Nitrate in Biological Fluids. *Anal Biochem* 1982;126:131-138.
- 12 Saltzman BE: Colorimetric Microdetermination of Nitrogen Dioxide in the Atmosphere. *Anal Chem* 1960;3:135-136.
- 13 Franken NAP, Rodermond HM, Stap J, Haveman J, van Bree C: Clonogenic assay of cells in vitro. *Nat Protoc*. 2006;1:2315-2319.
- 14 Ronot X, Benel L, Adolphe M, Mounolou JC: Mitochondrial analysis in living cells: the use of rhodamine 123 and flow cytometry. *Biol Cell* 1986;57:1-7.
- 15 de Godoy KF, de Almeida Rodolpho JM, Brassolatti P, de Lima Fragelli BD, de Castro CA, Assis M, Bernardi JC, Correia RO, Albuquerque YR, Speglich C, Longo E, Anibal FF: New Multi-Walled carbon nanotube of industrial interest induce cell death in murine fibroblast cells. *Toxicol Mech Methods* 2021;31:517-530.
- 16 Bhattacharya K, Mukherjee SP, Gallud A, Burkert SC, Bistarelli S, Bellucci S, Bottini M, Star A, Fadeel B: Biological interactions of carbon-based nanomaterials: From coronation to degradation. *Nanomedicine* 2016;12:333-351.
- 17 Yuan X, Zhang X, Sun L, Wei Y, Wei X: Cellular Toxicity and Immunological Effects of Carbon-based Nanomaterials. *Part Fibre Toxicol* 2019;16:1-27.
- 18 Fujita K, Fukuda M, Endoh S, Maru J, Kato H, Nakamura A, Shinohara N, Uchino K, Honda K: Size effects of single-walled carbon nanotubes on in vivo and in vitro pulmonary toxicity. *Inhal Toxicol* 2015;27:207-223.
- 19 Pulskamp K, Diabaté S, Krug HF: Carbon nanotubes show no sign of acute toxicity but induce intracellular reactive oxygen species in dependence on contaminants. *Toxicol Lett* 2007;168:58-74.
- 20 Gliniski A, Lima de Souza T, Zablocki da Luz J, Bezerra Junior AG, Camargo de Oliveira C, de Oliveira Ribeiro CA, Filipak Neto F: Toxicological effects of silver nanoparticles and cadmium chloride in macrophage cell line (RAW 264.7): An in vitro approach. *J Trace Elem Med Biol* 2021;68:126854.
- 21 Bacanlı M, Anlar HG, Başaran AA, Başaran N: Assessment of Cytotoxicity Profiles of Different Phytochemicals: Comparison of Neutral Red and Mtt Assays in Different Cells in Different Time. *Turk J Pharm Sci* 2017;14:95-107.

- 22 di Cristo L, Bianchi MG, Chiu M, Taurino G, Donato F, Garzaro G, Bussolati O, Berganaschi E: Comparative in vitro cytotoxicity of realistic doses of benchmark multi-walled carbon nanotubes towards macrophages and airway epithelial cells. *Nanomaterials* 2019;9:982.
- 23 Nahle S, Safar R, Grandemange S, Foliguet B, Lovera-Leroux M, Doumandji Z, Le Faou A, Joubert O, Rihn B, Ferrari L: Single wall and multiwall carbon nanotubes induce different toxicological responses in rat alveolar macrophages. *J Appl Toxicol* 2019;39:764-772.
- 24 Louro H, Pinhão M, Santos J, Tavares A, Vital N, Silva MJ: Evaluation of the cytotoxic and genotoxic effects of benchmark multi-walled carbon nanotubes in relation to their physicochemical properties. *Toxicol Lett* 2016;262:123-134.
- 25 Andersen AJ, Wibroe PP, Moghimi SM: Perspectives on carbon nanotube-mediated adverse immune effects. *Adv Drug Deliv Rev* 2012;64:1700-1705.
- 26 Moolgavkar SH, Brown RC, Turim J: Biopersistence, fiber length, and cancer risk assessment for inhaled fibers. *Inhal Toxicol* 2001;13:755-772.
- 27 Sabido O, Figarol A, Klein JP, Bin V, Forest V, Pourchez J, Fubini B, Cottier M, Tomatis M, Boudard D: Quantitative flow cytometric evaluation of oxidative stress and mitochondrial impairment in raw 264.7 macrophages after exposure to pristine, acid functionalized, or annealed carbon nanotubes. *Nanomaterials* 2020;10:319.
- 28 Sims CM, Hanna SK, Heller DA, Horoszko CP, Johnson ME, Montoro Bustos AR, Reipa V, Riley KR, Nelson BC: Redox-active nanomaterials for nanomedicine applications. *Nanoscale* 2017;9:15226-15251.
- 29 Fu PP, Xia Q, Hwang HM, Ray PC, Yu H: Mechanisms of nanotoxicity: Generation of reactive oxygen species. *J Food Drug Anal* 2014;22:64-75.
- 30 Basuroy S, Tcheranova D, Bhattacharya S, Leffler CW, Parfenova H: Nox4 NADPH oxidase-derived reactive oxygen species, via endogenous carbon monoxide, promote survival of brain endothelial cells during TNF-induced apoptosis. *Am J Physiol Cell Physiol* 2011;300:256-265.
- 31 de Almeida Rodolpho JM, de Godoy KF, Brassolatti P, de Lima Fragelli BD, de Castro CA, Assis M, Speglich C, Bernardi JC, Longo E, Anibal FF: Apoptosis and oxidative stress triggered by carbon black nanoparticle in the LA-9 fibroblast. *Cell Physiol Biochem* 2021;55:364-377.
- 32 Zhang T, Tang M, Kong L, Li H, Zhang T, Zhang S, Xue Y, Pu Y: Comparison of cytotoxic and inflammatory responses of pristine and functionalized multi-walled carbon nanotubes in RAW 264.7 mouse macrophages. *J Hazard Mater* 2012;219:203-212.
- 33 Özcan N, Karaman C, Atar N, Karaman O, Yola ML: A Novel Molecularly Imprinting Biosensor Including Graphene Quantum Dots/Multi-Walled Carbon Nanotubes Composite for Interleukin-6 Detection and Electrochemical Biosensor Validation. *ECS J Solid State Sci Technol*. 2020;9:121010.
- 34 Visalli G, Facciola A, Currò M, Laganà P, la Fauci V, Iannazzo D, Pistone A, Di Pietro A: Mitochondrial impairment induced by sub-chronic exposure to multi-walled carbon nanotubes. *Int J Environ Res Public Health* 2019;16:792.
- 35 Zeinabadi HA, Zarrabian A, Saboury AA, Alizadeh AMO, Falahati M: Interaction of single and multi wall carbon nanotubes with the biological systems: Tau protein and PC12 cells as targets. *Sci Rep* 2016;6:1-23.
- 36 Cheng WW, Lin ZQ, Wei BF, Zeng Q, Han B, Wei CX, Fand XJ, Hub CL, Liao LH, Huang JH, Yang X, Xi ZG: Single-walled carbon nanotube induction of rat aortic endothelial cell apoptosis: Reactive oxygen species are involved in the mitochondrial pathway. *Int J Biochem Cell Biol* 2011;43:564-572.
- 37 Liu Z, Dong X, Song L, Zhang H, Liu L, Zhu D, Song C, Leng X: Carboxylation of multiwalled carbon nanotube enhanced its biocompatibility with L02 cells through decreased activation of mitochondrial apoptotic pathway. *J Biomed Mater Res A* 2014;102:665-673.
- 38 Monian P, Jiang X: Clearing the final hurdles to mitochondrial apoptosis: Regulation post cytochrome C release. *Exp Oncol* 2012;34:185-191.
- 39 Wu H, Che X, Zheng Q, Wu A, Pan K, Shao A, Wu Q, Zhang J, Hong Y: Caspases: A molecular switch node in the crosstalk between autophagy and apoptosis. *Int J Biol Sci* 2014;10:1072-1083.
- 40 Qian QZ, Cao XK, Liu HY, Zheng GY, Qian QQ, Shen FH: TNFR/TNF- α signaling pathway regulates apoptosis of alveolar macrophages in coal workers' pneumoconiosis. *Oncotarget* 2018;9:1302-1310.
- 41 Samarghandian S, Nezhad M, Mohammadi G: Role of Caspases, Bax and Bcl-2 in Chrysin-Induced Apoptosis in the A549 Human Lung Adenocarcinoma Epithelial Cells. *Anticancer Agents Med Chem* 2014;14:901-909.

- 42 Kim WH, Song HO, Choi HJ, Bang HI, Choi DY, Park H: Ethyl Gallate Induces Apoptosis of HL-60 Cells by Promoting the Expression of Caspases-8, -9, -3, Apoptosis-Inducing Factor and Endonuclease G. *Int J Mol Sci* 2012;13:11912-11922.
- 43 Inserte J, Cardona M, Poncelas-Nozal M, Hernando V, Vilarrosa Ú, Aluja D, Parra VM, Sanchis D, Dorado DG: Studies on the role of apoptosis after transient myocardial ischemia: genetic deletion of the executioner caspases-3 and -7 does not limit infarct size and ventricular remodeling. *Basic Res Cardiol* 2016;111:1-10.
- 44 Green DR, Llambi F: Cell Death Signaling. *Cold Spring Harb Perspect Biol* 2015;7:a006080.
- 45 Zhou L, Forman HJ, Ge Y, Lunec J: Multi-walled carbon nanotubes: A cytotoxicity study in relation to functionalization, dose and dispersion. *Toxicol In Vitro* 2017;42:292-298.